Cellulose (2018) 25:593–606
https://doi.org/10.1007/s10570-017-1557-6

ORIGINAL PAPER

Enhanced swelling and multiple-responsive properties of gelatin/sodium alginate hydrogels by the addition of carboxymethyl cellulose isolated from pineapple peel

Hongjie Dai · Shiyi Ou · Yue Huang · Zhijun Liu · Huihua Huang

Received: 5 August 2017 / Accepted: 3 November 2017 / Published online: 8 November 2017

Abstract Natural polymers hydrogels were prepared by solution blending of gelatin, sodium alginate and carboxymethyl cellulose isolated from pineapple peel, and cross-linking with $CaCl_2$ and glutaraldehyde solutions. The prepared hydrogels were characterized by Fourier transform infrared spectroscopy, X-ray diffraction and field emission scanning electron microscope. The swelling behaviors and responsiveness to pH, salt and electric field were also investigated. The swelling dynamic mechanism of hydrogels agreed well with the Fickian diffusion and Schott's pseudo second order models. The addition of carboxymethyl cellulose enhanced the swelling ability of the hydrogels in the selected mediums and sensitivities to pH, salt and electric field. The electric response of the hydrogels showed pH-dependent, ionic strength-dependent and electric voltage-dependent. This multiple-responsive characteristic of the prepared hydrogels was conducive to application as potential biomaterials such as microsensors, actuators, artificial muscles and drug delivery systems.

Keywords Pineapple peel · Carboxymethyl cellulose · Hydrogel · Electric field · Multiple response

H. Dai · Y. Huang · Z. Liu · H. Huang (✉)
School of Food Science and Engineering, South China University of Technology, Guangzhou 510641, China
e-mail: fehhuang@scut.edu.cn

S. Ou
Department of Food Science and Engineering, Jinan University, Guangzhou 510632, China

Z. Liu
Guangdong Polytechnic of Science and Trade, Guangzhou 510430, China

Present Address:
H. Huang
No.381, Wushan Road, Tianhe District, Guangzhou City, Guangdong Province, China

Introduction

Until now, most low-cost agricultural byproducts or wastes such as straw, leaves, corn cob, and fruit peels, have still remained largely unutilized and been discarded as wastes (Dai and Huang 2016; Zhao et al. 2013). Pineapple (*Ananas comosus* L. Merryl) is a typical and popular tropic fruit with total production of 16–19 million tonnes per year around the world. Besides consuming as fresh fruit, pineapple can be processed into can food and food complements used in desserts, salads, fruit cocktail, jam, juice combinations, and also available for bromelain extraction (Dai and Huang 2017a, b; Foo and Hameed 2012; Hu et al. 2010; Wan et al. 2016). Unfortunately, pineapple peel, accounting for 35% of the total pineapple weight, is discarded with little or no economic value during the pineapple processing, subsequently resulting in a

potential risk towards the environments and ecosystems (Dai and Huang 2017a, b; Hu et al. 2010). Therefore, taking full advantage of pineapple peel is of great practical significance. Pineapple peel principally consists of cellulose, hemi-cellulose, lignin and pectin, in which cellulose accounts for 20–25% of the dry weight and has the tremendous potential for producing cellulosic based-materials (de Almeida et al. 2016; Rattanapoltee and Kaewkannetra 2014). In our previous studies, we have successfully prepared the pineapple peel cellulose and a series of pineapple peel cellulose based-hydrogels for the applications of drug release, dye and heavy metal adsorption, and enzyme immobilization (Dai and Huang 2016, 2017a, b; Dai et al. 2017; Hu et al. 2010, 2013). However, there is still an urgent need for more effective use of pineapple peel cellulose and its hydrogels.

Cellulose, the most abundant renewable carbon resource available on earth, consists of a straight chain linked by anhydroglucopyranose units (AGU) via β-(1 → 4) glycosidic linkage and contains numerous intra- and inter-molecular hydrogen bonds (Dai and Huang 2017a, b; Saelo et al. 2016). With the increasing concerning for environmentally friendly and biocompatible products, numerous cellulose-based materials are being developed over a broad range of applications due to its nontoxicity, biodegradation, biocompatibility, superior thermal and mechanical properties as well as inexhaustibility (Dai and Huang 2016). However, due to its indissolubility in most common solvents, cellulose is generally converted into available derivatives by etherification prior to further processing (Zhang et al. 2017). Herein, carboxymethyl cellulose (CMC) is one of the most common derivates obtained by the carboxymethylation of the hydroxyl groups of cellulose (Lin et al. 2015). Due to its solubility, biocompatibility and biodegradation, CMC exhibits the greatest potential use in food, paper, cosmetics, textile, pharmaceutical and paint industries (Dai and Huang 2017a, b; Dai et al. 2017; Sommer et al. 2016).

Hydrogels are defined as the three-dimensional hydrophilic networks, which are capable of absorbing large amounts of water and retaining the swollen state instead of being dissolved in medium (Mahdavinia et al. 2016). Especially, by changing their volume or shape reversibly, intelligent hydrogels can respond to external stimuli such as the changes in temperature, pH, salt, light, electric field and multiple stimuli (Bekin et al. 2014; Dai and Huang 2017a, b; Tungkavet et al. 2015). Based on these responsive characteristic, smart hydrogels have been intensively explored for applications in various fields, such as drug delivery (Constantin et al. 2017), enzyme immobilization (Ullah et al. 2015), 3D bioprinting (Gou et al. 2014), adsorbents (Ren et al. 2016), and agriculture industry (Zhang et al. 2017). Compared with synthetic polymers such as acrylic acid, acrylamide and poly(ethylene glycol), the smart hydrogels based on natural polymers possess advantages such as high hydrophilicity, biocompatibility, nontoxicity and biodegradability and subsequently obtain more attention (Dai and Huang 2017a, b; Thakur et al. 2014; Yu et al. 2016). On the smart hydrogels, electric-sensitive hydrogels have inspired tremendous interest recently due to their merits of easy control by electric signal and energy conversion from electric to mechanical energy (Bekin et al. 2014; Tian et al. 2010). Compared with the electric-sensitive hydrogels based on synthetic polymers, electric-sensitive hydrogels based on natural polymers exhibit better potential access to sensors, artificial muscles, membrane separation devices, and drug delivery systems due to their biocompatibility and non-toxicity (Tian et al. 2010).

Among the most natural polymers, sodium alginate, a non-toxic biodegradable polyanionic copolymer extracted from marine brown algae, is a linear chain of α-L-guluronic acid (G) and β-D-mannuronic acid (M) residues joined by 1,4-glucosidic linkages (Ibrahim et al. 2014). Due to its remarkable gelation characteristic in the presence of divalent cations and the advantages of hydrophilicity, biocompatibility and biodegradability, sodium alginate based-hydrogels have captured tremendous research interest in various application fields recently (Işiklan 2006; Mahdavinia et al. 2016; Ren et al. 2016; Saarai et al. 2013; Samanta and Ray 2014). Gelatin is a biopolymeric-protein obtained by partial hydrolysis of animal collagen from bones and skin regarded as wastes during animal slaughtering and processing (Mu et al. 2012). Besides low-cost and abundance, gelatin exhibits the characteristics of biocompatibility, hydrophilicity, biodegradability and nontoxicity (Jana et al. 2016). By virtue of these attractive advantages, gelatin has been broadly utilized as a natural raw material of hydrogels recently (Jana et al. 2016; Mu et al. 2012; Thu and Ng 2013; Tungkavet et al. 2015).

However, the hydrogels based on neat sodium alginate or gelatin still suffer from significant disadvantages of poor mechanical strength and low thermal stability (Badawy et al. 2017; Saarai et al. 2013). In addition, rapid dissolution of neat gelatin-based hydrogels in aqueous environment also limits its application (Jana et al. 2016). It is also reported that neat sodium alginate-based hydrogel is mainly sensitive to the environmental pH change and nearly absent in electrical responsiveness under electric field (Shi et al. 2015). To overcome these limitations, some kinds of synthetic or natural polymers have been added to form composite hydrogels by chemical and/or physical cross-linking. Based on the above description, in the present study, the multi-component hydrogels based on sodium alginate, gelatin and carboxymethyl cellulose were synthesized by double-crosslinking with $CaCl_2$ and glutaraldehyde, and based on the characterization of the structure and morphology by Fourier transform infrared spectroscopy (FTIR), X-ray diffraction (XRD), and scanning electron microscopy (SEM), the swelling behavior and responsiveness to pH, salt and electric field of the prepared hydrogels were investigated and compared.

Materials and methods

Materials and reagents

Pineapple peel was collected from a local pineapple processing factory (Guangzhou City, China), consisting of 23.67% cellulose, 15.61% hemicellulose, 6.87% lignin, 5.71% pectin and 2.37% ash (Dai and Huang 2017a, b). Pineapple peel carboxymethyl cellulose (PCMC) was prepared and obtained according to our previous study (Dai and Huang 2017a, b). Gelatin (GL) was supplied by BDH Chemicals Co., Ltd (Poole City, England), approximately 150 Bloom, from pig skin. Sodium alginate (SA) was provided by Tianjin Kermel Chemical Reagent Co., Ltd. (Tianjin City, China). Glutaraldehyde (25%, w/v, aqueous solution) was provided by Sinopharm Chemical Reagent Co., Ltd. (Shanghai, China). All other chemicals and solvents used in this study were of analytical grade and solutions were prepared with distilled water.

Hydrogels preparation

Briefly, GL solutions were prepared by addition of 4.0 g of GL into 100 mL of distilled water and the mixtures were stirred mechanically at 60 °C until to complete dissolution of GL. Then, as the different treatments, three different proportions of SA and PCMC, including: (1.6 g SA), (1.2 g SA + 0.4 g PCMC) and (0.8 g SA + 0.8 g PCMC), were added to the GL solutions and stir-treated to form a homogeneous solution respectively. After removing the air bubbles by sonication, the resulting solutions were poured into circular moulds such as 24-well plate and Petri dish and immersed in 0.1 mol/L $CaCl_2$ solution for 4 h to form the insoluble and stable hydrogels. After washing with distilled water, further cross-linking was achieved by treatment with 0.5% (v/v) of glutaraldehyde solution for 2 h, then washing with distilled water and freeze-drying for the hydrogels were performed. The prepared hydrogels were now available for the following study and coded according to their treatments with the initial compositions, namely GL4.0/SA1.6, GL4.0/SA1.2/PCMC0.4 and GL4.0/SA0.8/PCMC0.8. The preparation process of the hydrogels is briefly described in Scheme 1a, and the photographs of the prepared hydrogels are shown in Scheme 1b (Petri dish as a mold) and Scheme 1c (24-well plate as a mold).

Characterization

FTIR spectra of the samples were recorded on a FTIR spectrometer (Vector 33, Bruker, Germany) within the frequency range of 4000–500 cm^{-1} at a resolution of 4 cm^{-1}. XRD patterns of the samples were recorded on an X-ray diffractometer (D8 ADVANCE, Bruker, Germany) with Cu-Ka radiation ($\lambda = 0.15418$ nm) at 40 kV and 40 mA. The XRD data were collected in the region of the diffraction angle (2θ) from 4° to 50° with a scanning speed of 2°/min. The surface morphologies of the samples were investigated using a scanning electron microscope (S-3700 N, Hitachi, Japan). Prior to observation, the surface of the tested samples was sputter-coated with gold using a sputter coater (Cressington 108 auto, Watford, UK).

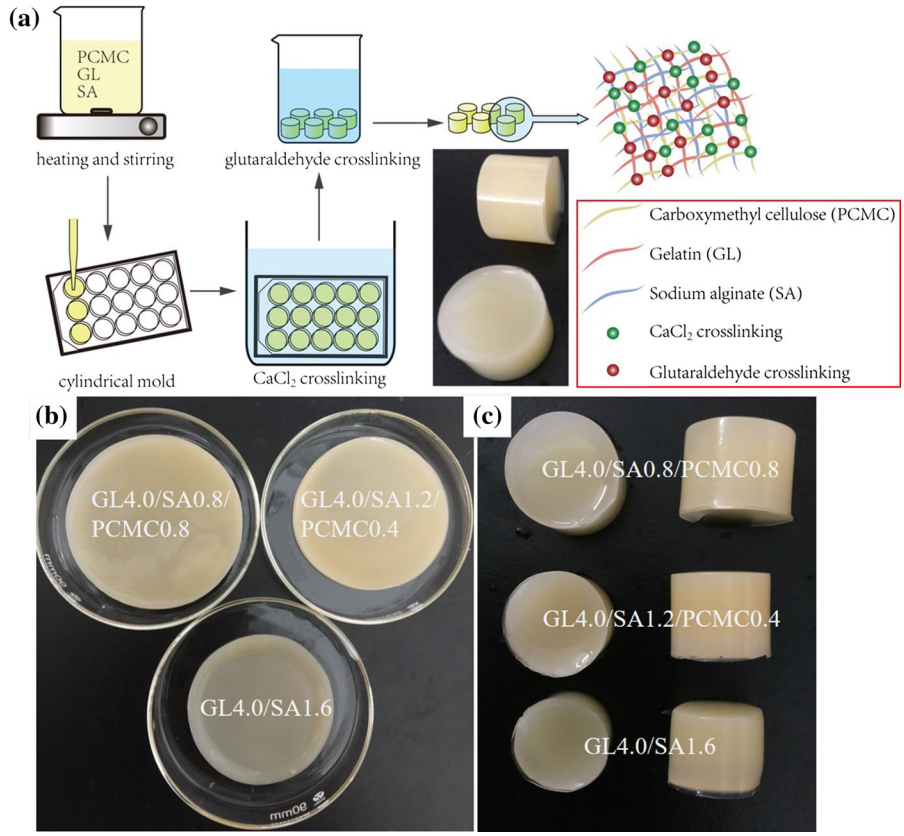

Scheme 1 The brief hydrogel preparation process and the photographs of the hydrogels GL4.0/SA1.6, GL4.0/SA1.2/PCMC0.4 and GL4.0/SA0.8/PCMC0.8 prepared using different molds

Swelling kinetics of the prepared hydrogels

In this study, the swelling ratio (*SR*) of the prepared hydrogels in distilled water and 0.9% NaCl solution was investigated using the gravimetric method. 20 mg of the dried hydrogels was completely immersed in excess distilled water or 0.9% (w/v) NaCl solution at room temperature. After preset time intervals, the swollen hydrogels were taken from the swelling medium and weighed immediately after the removal of the excess surface water using filter paper. The *SR* of the hydrogels at a specified time can be obtained using Eq. 1.

$$SR(\mathrm{g/g}) = \frac{W_t - W_d}{W_d} \quad (1)$$

where *SR* (g/g) is the swelling ratio defined as the grams of absorbed water per gram of the dry hydrogels; W_t (g) and W_d (g) are the weights of swollen hydrogels at time *t* (min) and dried hydrogels, respectively.

Swelling of the prepared hydrogels in various pH solutions

50 mg of the dried hydrogels was immersed in different solutions at pH 2.0, 7.0 and 12.0 respectively. The ionic strengths of all the solutions were adjusted to 0.1 mol/L by adding appropriate amounted NaCl. To investigate the pH sensitivity of the prepared hydrogels, the swelling kinetics at various pH solutions (pH 2.0, 7.0 and 12.0) were also recorded and compared.

Swelling of the prepared hydrogels in various saline solutions

To investigate the influence of salt species and strengths on the swelling behaviors of the prepared hydrogels, the swelling abilities of the hydrogels were studied in NaCl and $FeCl_3$ solutions respectively with various concentrations ranged from 0.02 to 0.1 mol/L.

Bending behavior of the prepared hydrogels under electric stimulus

To evaluate the bending behavior of the prepared hydrogels under DC electric field, a Petri dish equipped with two parallel graphite plate electrodes was immersed in NaCl aqueous solution as the electrolyte solution. The gap between the electrodes was set 45 mm. Prior to measurement, the dried hydrogels were immersed in the selected NaCl solution for 24 h and were cut into identical sheets with the dimensions of 20 × 5 × 2 mm. The swollen hydrogels were fixed at the middle of the electrodes. Measures of the bending degree of the hydrogels were performed by attaching a full-circle protractor on the bottom of Petri dish. When an electric stimulus was applied, the degrees of bending (θ) were measured by reading the deviated angle from the vertical position.

Results and discussion

Characterization

FTIR analysis

The FTIR spectra of the prepared hydrogels GL4.0/SA1.6, GL4.0/SA1.2/PCMC0.4, GL4.0/SA0.8/PCMC0.8 and their original components, including GL, SA and PCMC are displayed in Fig. 1. For GL, the bands at 3493, 1651, 1533 and 1230 cm^{-1} were attributed to the N–H stretching vibration, amide I vibration, amide II bending vibration and amide III vibration, respectively (Devi and Kakati 2013; Piao and Chen 2017). For SA, the characteristic bands at 3351, 1625 and 1426 cm^{-1} were assigned to the O–H stretching, asymmetric stretching of –COO groups and symmetric stretching of –COO groups, respectively (Devi and Kakati 2013; Samanta and Ray 2014).The absorption bands at 820–1100 cm^{-1} were ascribed to the symmetric stretching of the C–C, C–H, and C–O–C skeletal vibrations of the glucose units and/or the polysaccharide structure (Mas Haris and Raju 2014). For PCMC, the bands at 3460, 2900 and 1053 cm^{-1} were ascribed to the stretching vibrations of O–H, C–H and C–O–C groups, respectively (Dai et al. 2017). The band at 1322 cm^{-1} was due to the bending vibration of O–H. The very intense bands at 1653 and 1423 cm^{-1} were corresponded to the stretching vibration of –COO and its salt forms, corresponding to the typical adsorption of carboxymethyl cellulose (Dai and Huang 2017a, b; Yadav et al. 2014). Compared GL, SA and PCMC in the spectrum with the prepared hydrogels (GL4.0/SA1.6, GL4.0/SA1.2/PCMC0.4 and GL4.0/SA0.8/PCMC0.8), it was observed that the band for O–H stretching vibration became broader and flatter, and showed increased intensity with the increase of PCMC content, suggesting that the extensive formation of hydrogen bonds probably among GL, SA and PCMC during the hydrogels network. The band at 1680 cm^{-1} was the characteristic of imine stretching vibrations corresponding to the reaction between $–NH_2$ groups of GL and –CHO groups of glutaraldehyde (Işiklan 2006). The band for the –COO symmetric stretching exhibited a slight shift from 1426 cm^{-1} (for SA) to 1445 cm^{-1} (for the hydrogels) with the decreased intensity, suggesting the presence of the ionic binding between the Ca^{2+} and –COO of SA (Saarai et al. 2013).

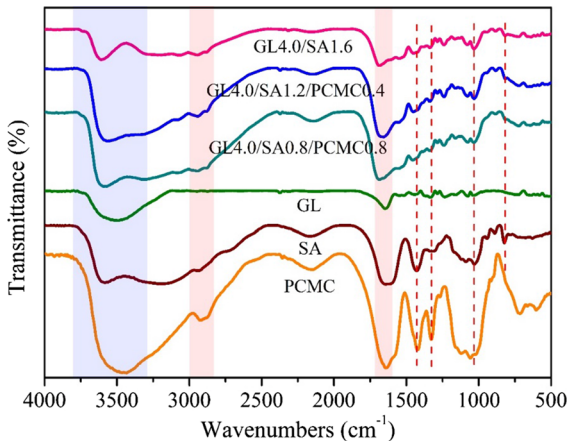

Fig. 1 FT-IR spectra of GL, SA, PCMC, and the prepared hydrogels GL4.0/SA1.6, GL4.0/SA1.2/PCMC0.4 and GL4.0/SA0.8/PCMC0.8

XRD analysis

The XRD spectra of the prepared hydrogels GL4.0/SA1.6, GL4.0/SA1.2/PCMC0.4, GL4.0/SA0.8/PCMC0.8 and their original components, including GL, SA and PCMC are shown in Fig. 2. GL showed a typical broad diffraction peak at $2\theta = 20.7°$ and a relative weak peak at $2\theta = 7.8°$. SA showed a strong diffraction peak at $2\theta = 13.5°$ accompanied by a weak

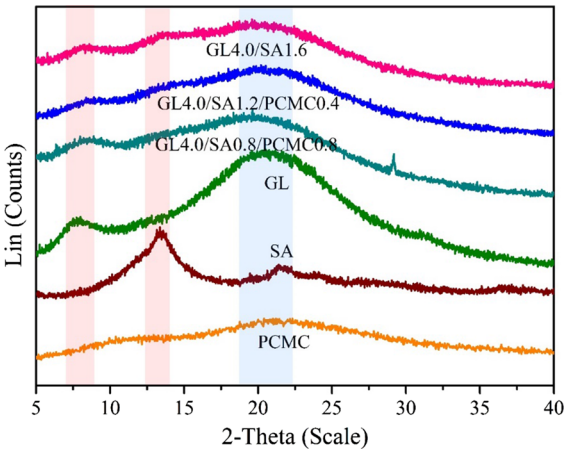

Fig. 2 XRD patterns of GL, SA, PCMC, and the prepared hydrogels GL4.0/SA1.6, GL4.0/SA1.2/PCMC0.4 and GL4.0/SA0.8/PCMC0.8

peak centered at $2\theta = 21.6°$, indicating its amorphous nature (Devi and Kakati 2013). Similar positions of the relevant peaks in the diffractograms for GL and SA were also reported by other authors (Dong et al. 2006; Thu and Ng 2013). As for PCMC, our previous study showed that pineapple peel cellulose displayed characteristic crystalline peaks of cellulose I at $2\theta = 21.8°$, 15.3° and 34.6° (Dai and Huang 2017a, b). However, after carboxymethylation of pineapple peel cellulose, only a broad and weak diffraction peak at $2\theta = 22.1°$ was observed for PCMC, indicating carboxymethylation induces the low crystallinity of PCMC and the possible shift of crystalline structure from cellulose I to cellulose II (Dai and Huang 2017a, b; Dai et al. 2017). After formation of hydrogels, GL4.0/SA1.6, GL4.0/SA1.2/PCMC0.4 and GL4.0/SA0.8/PCMC0.8 showed a very broad peak but decreased in intensity at $2\theta = 19.8°$, indicating the conversion from the original crystalline structure of GL, SA and PCMC to the characteristics of amorphous. Furthermore, with the increase of proportion of PCMC and decrease of SA in the hydrogels, the typical peak of SA at $2\theta = 13.5°$ disappeared and the peak of GL at $2\theta = 7.8°$ shifted to $2\theta = 8.5°$. This disappearance and shift may be due to the results of cross-linked reaction and presence of strong interactions among SA, GL and PCMC, especially electrostatic attraction (Thu and Ng 2013).

SEM analysis

The SEM images of GL, SA, PCMC, and the prepared hydrogels GL4.0/SA1.6, GL4.0/SA1.2/PCMC0.4 and GL4.0/SA0.8/PCMC0.8 are shown in Fig. 3. As can be seen from Fig. 3a–c, as the original components of the prepared hydrogels, GL (Fig. 3a) exhibited an obvious block-like structure with smooth surfaces. Unlike the block-like structure of GL, SA (Fig. 3b) showed an agglomerated and irregular rod-like morphology with rough surfaces. As observed in Fig. 3c, PCMC revealed a fiber-like structure with relatively smooth surfaces. Compared with the original components, as shown in Fig. 3d–f, the prepared hydrogels exhibited a uniform surface structure. It can be clearly observed that the GL4.0/SA1.6 (Fig. 3d) only showed a smooth and non-porous surface. However, after the introduction of PCMC, as depicted in Fig. 3e, f, the surfaces of GL4.0/SA1.2/PCMC0.4 and GL4.0/SA0.8/PCMC0.8 possessed many hole-shaped wrinkles whose quantity increased with the increase of PCMC content. Significantly, these wrinkles could provide an increase in surface area of the prepared hydrogels, leading to the easy diffusion of aqueous fluid into the hydrogel network and a higher swelling capacity (Wang et al. 2011).

Swelling kinetics and comparison between the prepared hydrogels

The swelling kinetics of the prepared hydrogels GL4.0/SA1.6, GL4.0/SA1.2/PCMC0.4 and GL4.0/SA0.8/PCMC0.8 in distilled water and 0.9% NaCl solution are displayed in Fig. 4a, b, respectively. As clearly observed from the figure, the swelling capacity of the prepared hydrogels was significantly improved with the increased content of PCMC. The enhanced swelling capacity may be ascribed to the abundance of highly hydrophilic hydroxyl group and carboxymethyl group of PCMC, which favor enhanced affinity of the hydrogels network to water molecules (Chang et al. 2010). As depicted in Fig. 4a, b, the swelling ratio increased drastically during the initial 120 min, and then became slower until reaching a plateau. After the addition of PCMC, in comparison with GL4.0/SA1.6 (prepared without addition of PCMC) and GL4.0/SA0.8/PCMC0.8, the corresponding equilibrium swelling ratio increased from 9.76 to 11.79 g/g in distilled water and from 10.59 to 12.51 g/g in 0.9%

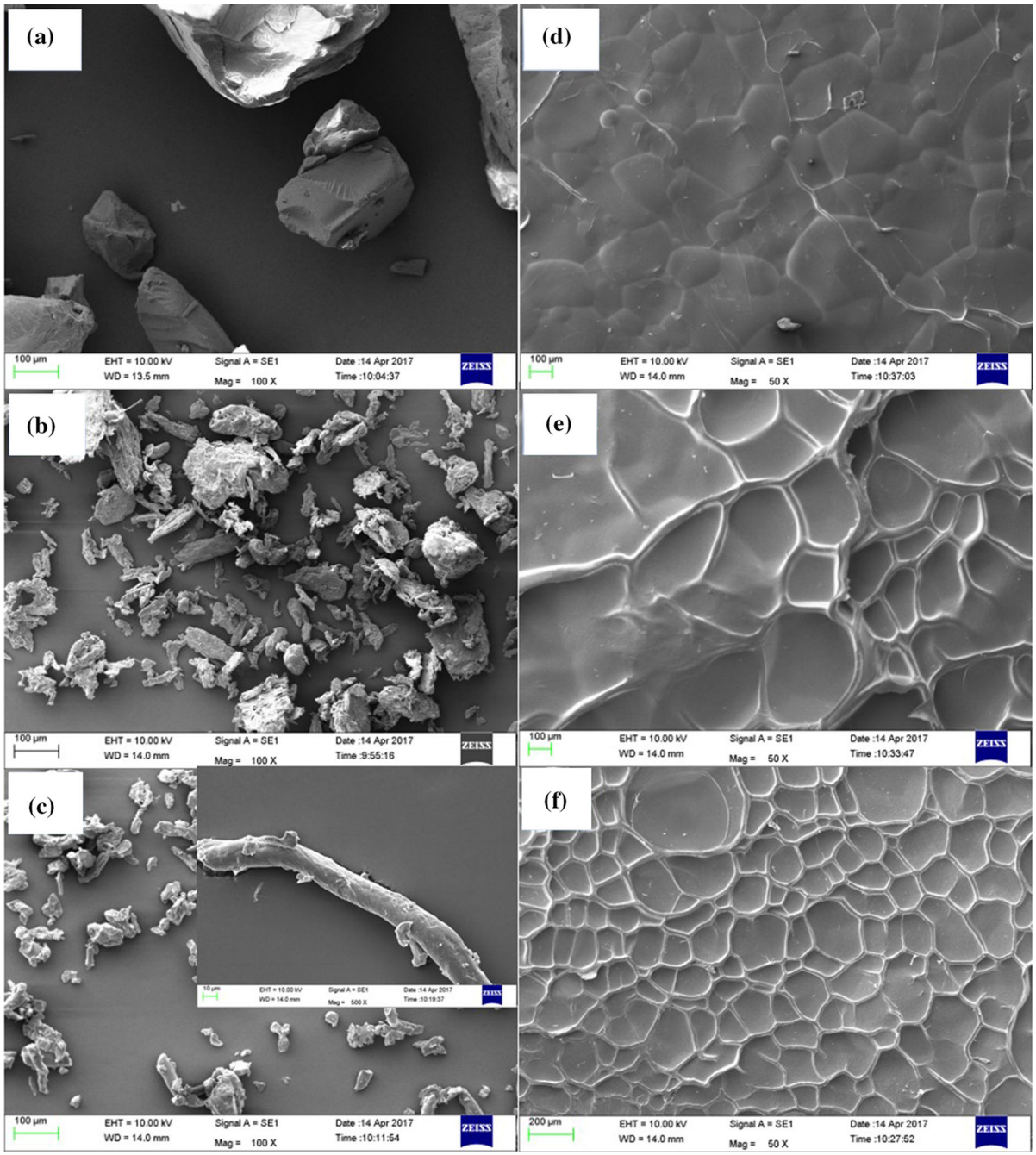

Fig. 3 SEM images of GL (**a**), SA (**b**), PCMC (**c**), and the prepared hydrogels GL4.0/SA1.6 (**d**), GL4.0/SA1.2/PCMC0.4 (**e**) and GL4.0/SA0.8/PCMC0.8 (**f**)

NaCl solution, indicating that the addition of PCMC into the hydrogels can enhance the swelling capacity. Interestingly, compared with the swelling in distilled water, the prepared hydrogels showed a slightly higher swelling ratio in 0.9% NaCl solution.

To investigate the dynamic swelling behaviors of the hydrogels, the whole swelling processes were analyzed by the Fickian diffusion for the penetration of the solvent molecules into the void spaces in the network at the initial swelling stage and the Schott's

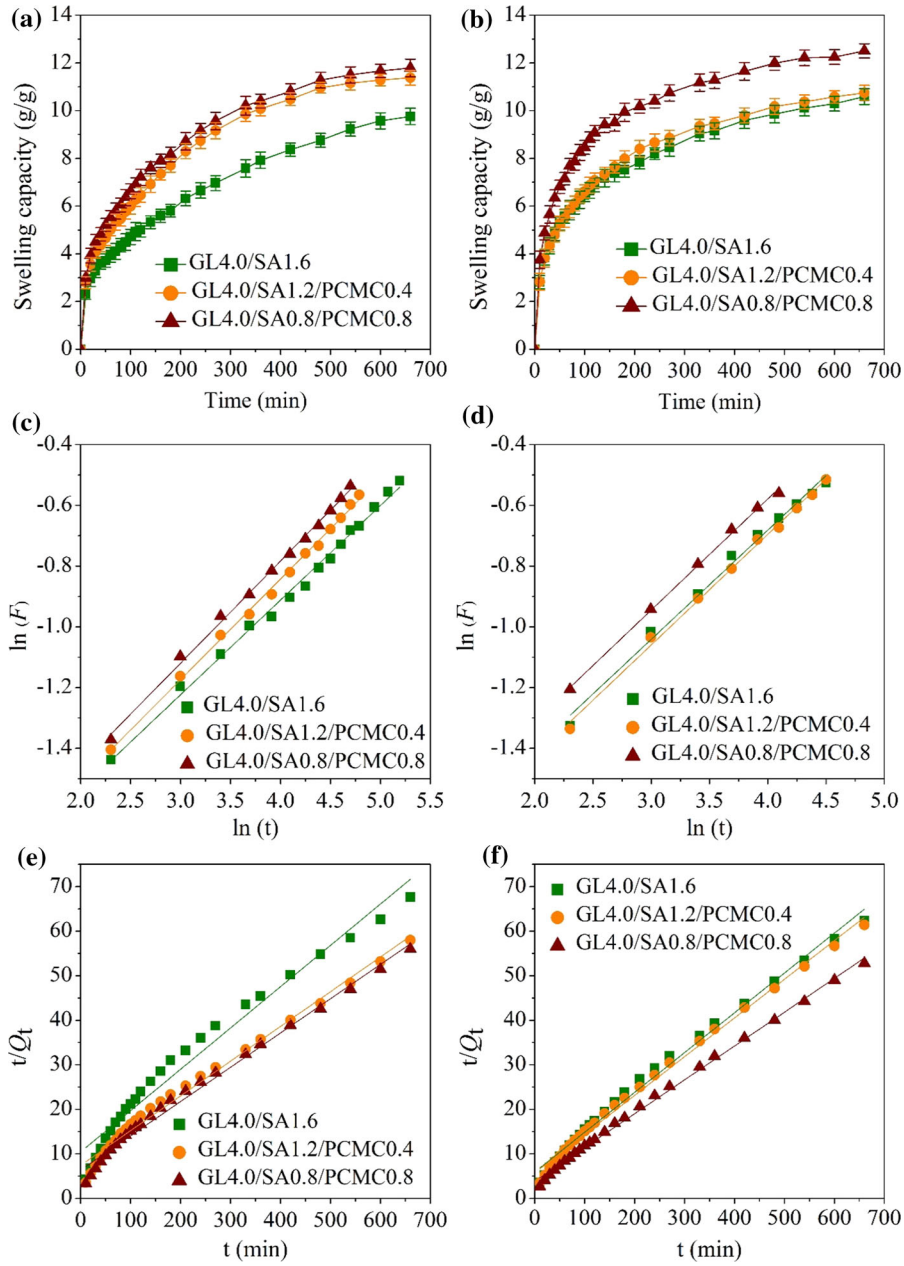

Fig. 4 Swelling kinetic curves of the prepared hydrogels GL4.0/SA1.6, GL4.0/SA1.2/PCMC0.4 and GL4.0/SA0.8/PCMC0.8 in distilled water (**a**) and 0.9% NaCl solution (**b**), and the plots of ln (F) against ln (t) for the hydrogels in distilled water (**c**) and 0.9% NaCl solution (**d**) as well as the plots of t/Q_t against t for the hydrogels in distilled water (**e**) and 0.9% NaCl solution (**f**)

second-order-kinetic model for the subsequent relaxation of the polymeric chains, respectively.

At the initial swelling stage (about 60% of the maximum water uptake), the Fickian diffusion model was applied to describe the penetration mechanism and it can be expressed as Eq. 2 (Dai and Huang 2017a, b; Lima-Tenório et al. 2015).

$$F = \frac{M_t}{M_e} = Kt^n \quad (2)$$

where F represents the fractional uptake at a given time t (min); M_t (g) and M_e (g) are the weights of water absorbed at the given time t and equilibrium during swelling process, respectively; K is the characteristic constant of the hydrogels, and n is the diffusional exponent of the solvent. In the cases of $n < 0.5$, Fickian diffusion is dominant, where the water transport was governed by a simple concentration gradient. In the cases of $0.5 < n < 1$, non-Fickian

diffusion is dominant, where the water uptake was controlled collaboratively by water diffusion and relaxation of polymer chains. In the cases of $n > 1$, the relaxation of polymer chains would control the diffusion system (anomalous diffusion). Plotting with ln (F) versus ln (t) for the prepared hydrogels swelling in distill water and 0.9% NaCl solution are shown in Fig. 4c, d respectively. The corresponding n, K and R^2 of the hydrogels were calculated from the slope and intercept of the plots and listed in Table 1. The plots displayed straight lines with perfect linear correlation coefficient ($R^2 > 0.99$), suggesting the effectiveness of the Fickian diffusion model. The n values were all below 0.5, indicating the characteristic of Fickian diffusion behavior during the initial swelling stage in distilled water or 0.9% NaCl solution. As listed in Table 1, a slight higher n value was observed with the increase of PCMC content in hydrogels, implying that PCMC can accomplish easier relaxation of polymer chains for the water uptake.

For the whole swelling process, the Schott's second-order kinetic model was applied and described using Eq. 3 (Schott 1992).

$$\frac{t}{Q_t} = \frac{1}{kQ_e^2} + \frac{1}{Q_e}t \quad (3)$$

where Q_e (g/g) is the swelling ratio of hydrogels at theoretic equilibrium condition, Q_t (g/g) is the swelling ratio at a given time t (min), k (g/g min) is the initial swelling rate constant. The fitting of the experimental data by the Schott's second-order kinetic model was evaluated by the coefficient of determination (R^2). Based on the experimental data, the plots using t/Q_t versus t are shown in Fig. 4e, f, and the corresponding R^2, k and the swelling ratio ($Q_{e,cal}$, g/g) were calculated by linear regression and listed in Table 1. As shown in Fig. 4e, f, the plots presented straight lines with good linear correlation coefficient ($R^2 > 0.97$–0.99), confirming the well-fitting of data by second-order kinetic. The $Q_{e,cal}$ values calculated from the swelling kinetic model were close to the experimental values ($Q_{e,exp}$, g/g), suggesting that the Schott's second-order kinetic model was suitable for describing the entire swelling kinetic behaviors of the prepared hydrogels.

Swelling comparison between the prepared hydrogels in NaCl and $FeCl_3$ solutions

To evaluate salt sensitivity of the hydrogels, the swelling capacities of GL4.0/SA1.6, GL4.0/SA1.2/PCMC0.4 and GL4.0/SA0.8/PCMC0.8 in NaCl and $FeCl_3$ solutions at various concentrations (0.02–0.1 mol/L) were depicted and compared, as shown in Fig. 5. As can be clearly seen, the prepared hydrogels significantly exhibited lower swelling capacity in $FeCl_3$ than NaCl solution due to the increase of ionic charge ($Fe^{3+} > Na^{+}$). The swelling ratios of GL4.0/SA1.6, GL4.0/SA1.2/PCMC0.4 and GL4.0/SA0.8/PCMC0.8 in 0.1 mol/L NaCl solution were 9.47, 10.15 and 12.19 g/g, respectively, while their swelling ratios in 0.1 mol/L $FeCl_3$ solution significantly decreased to 2.15, 2.41 and 2.66 g/g, respectively. The swelling capacity also decreased appreciably with the increase of NaCl or $FeCl_3$ concentration. When NaCl or $FeCl_3$ concentration increased from 0.02 to 0.1 mol/L, the swelling ratios of GL4.0/SA0.8/PCMC0.8 decreased from 16.31 to 12.19 g/g in NaCl solution, and 4.49 to 2.66 g/g in $FeCl_3$. These ionic charge-dependence and ionic strength-dependence of the prepared hydrogels in swelling demonstrated the

Table 1 Swelling kinetic parameters for the prepared hydrogels GL4.0/SA1.6, GL4.0/SA1.2/PCMC0.4 and GL4.0/SA0.8/PCMC0.8 in distilled water and 0.9% NaCl solution

Hydrogels	Fickian diffusion model			Schott's second-order kinetic model			
	R^2	K	n	$Q_{e,exp}$	R^2	$Q_{e,cal}$	$k \times 10^3$
In distilled water							
GL4.0/SA1.6	0.9945	0.1156	0.3114	515.24	0.9709	10.79	0.82
GL4.0/SA1.2/PCMC0.4	0.9974	0.1145	0.3313		0.9872	12.84	0.82
GL4.0/SA0.8/PCMC0.8	0.9972	0.1192	0.3359	420.17	0.9906	13.01	0.93
In 0.9% NaCl solution							
GL4.0/SA1.6	0.9928	0.1201	0.3595		0.9925	11.19	1.35
GL4.0/SA1.2/PCMC0.4	0.9968	0.1163	0.3641	37.89	0.9949	11.51	1.31
GL4.0/SA0.8/PCMC0.8	0.9984	0.1298	0.3658	28.03	0.9974	13.16	1.50

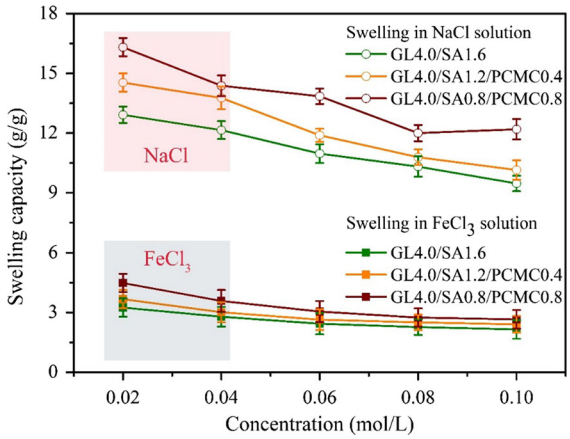

Fig. 5 Swelling behaviors of the prepared hydrogels GL4.0/SA1.6, GL4.0/SA1.2/PCMC0.4 and GL4.0/SA0.8/PCMC0.8 in NaCl and $FeCl_3$ solutions

prepared hydrogels have the salt sensitivity. The shrinking behavior of the prepared hydrogels in $FeCl_3$ solution could be attributed to the reduced osmotic pressure difference between the interior polymer network and the external solution, which is determined by the ionic interactions between mobile ions and the fixed charges in salt solutions (Dai and Huang 2017a, b; Huang et al. 2013) According to Donnan osmotic pressure equilibrium, at high salt concentration, a shrinking swelling behavior can be easily induced due to the more movable counterions and low osmotic pressure difference between interior and exterior of the hydrogel (Tang et al. 2014).This behavior also can be explained by Flory's equation (Lanthong et al. 2006).

$$Q^{5/3} \approx \frac{(i/2V_u S^{1/2})^2 + (1/2 - x_1)V_1}{V_E/V_0} \quad (4)$$

where Q represents the swelling degree of the polymer, i/V_u is the charge density of the polymer, S is the ionic strength of solution, $(1/2 - x_1)/V_1$ is the affinity between polymer and solution, V_E/V_0 is the crosslinking density of the polymer. Based on the Flory's equation, the swelling degree of the polymer in salt solutions is monovalent > trivalent cations ($Na^+ > Fe^{3+}$), agreeing well with the swelling capacities of the hydrogels in NaCl and $FeCl_3$ solutions.

Swelling comparison between the prepared hydrogels in various pH solutions

To analyze pH sensitivity of the prepared hydrogels, the swelling kinetics and pH-dependent swelling behaviors of GL4.0/SA1.6, GL4.0/SA1.2/PCMC0.4 and GL4.0/SA0.8/PCMC0.8 in various pH solutions (pH 2.0, 7.0 and 12.0 respectively) were investigated and compared. As clearly displayed in Fig. 6, there existed a noticeable increase in the dynamic swelling curves from pH 2.0 to 12.0. The prepared hydrogels swelled very little at acidic medium (pH 2.0) but much more in neutral (pH 7.0) and alkaline medium (pH 12.0). For example, GL4.0/SA0.8/PCMC0.8 only showed the swelling ratio 5.32 g/g at pH 2.0, significantly lower than 10.44 g/g at pH 7.0 and 18.48 g/g at pH 12.0. The swelling was rapid up within 30 min in all solutions and reached the platform after 60 min at pH 2.0 and 200 min at pH 7.0 and 12.0. The evident pH-dependent swelling behaviors confirmed the pH-sensitive characteristic of the prepared hydrogels. Compared with GL4.0/SA1.6, GL4.0/SA1.2/PCMC0.4 and GL4.0/SA0.8/PCMC0.8 also showed improvement in swelling capacity due to the addition of PCMC. Due to the characteristics of anionic polymers, under the acidic conditions, a screening effect of the counter ions, i.e. Cl^- in the swelling medium, prevented an efficient repulsion, leading to a remarkable hydrogel collapsing. Meanwhile, due to the protonation of –COO– groups, the electrostatic repulsion among –COO– was reduced, consequently resulting in a decreased swelling ratio (Dai and Huang 2017a, b; Saarai et al. 2013). Furthermore, the amine groups of GL can be positively charged at lower pH and complex with alginate which is negatively charged, leading to the formation of more stable state (Devi and Kakati 2013). As the external pH increased, the electrostatic repulsion was enhanced owing to the ionization of –COOH groups, so the hydrogels network got more expanded and swelled more (Zhang et al. 2015). In such system, hydrogen bonding and a combination of attractive or repulsive electrostatic interactions were responsible for the pH-dependent behaviors of the hydrogels.

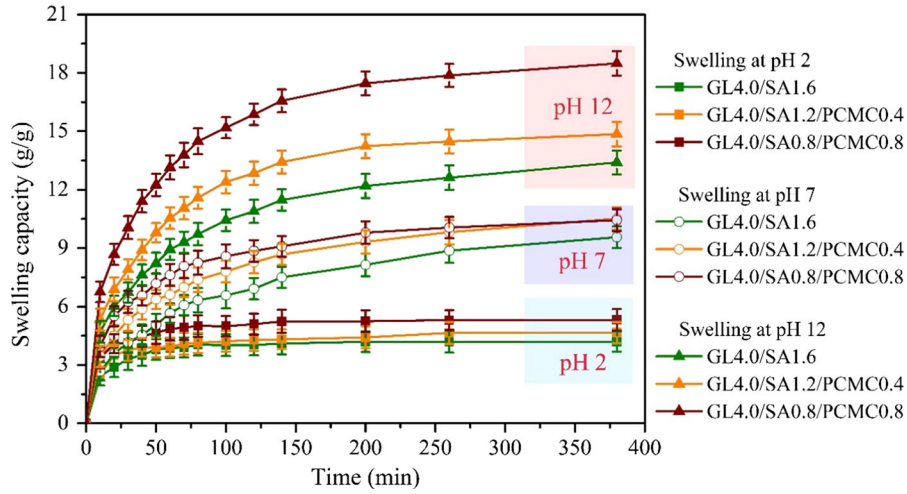

Fig. 6 Swelling kinetic curves for the prepared hydrogels GL4.0/SA1.6, GL4.0/SA1.2/PCMC0.4 and GL4.0/SA0.8/PCMC0.8 in various pH solutions (pH 2.0, 7.0 and 12.0)

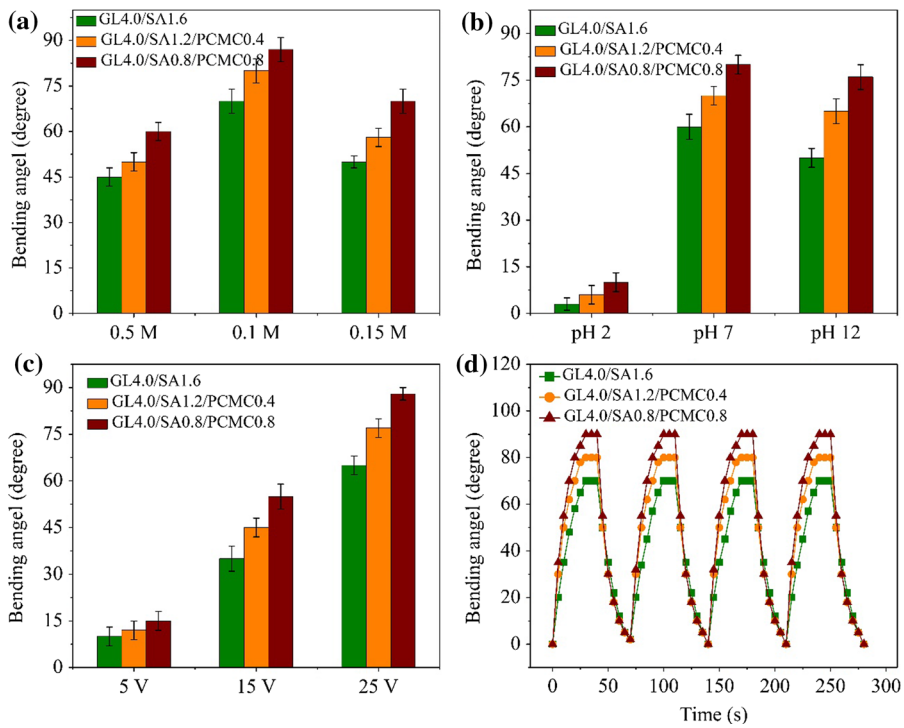

Fig. 7 The influences of ionic strength at 25 V and pH 7.0 (**a**), pH value at 0.1 M and 25 V (**b**) and electric voltage at pH 7.0 and 0.1 M (**c**) on the bending behaviors of the prepared hydrogels and the reversible bending behaviors of the hydrogels by alternately applying electric voltage of 25 V every 30 s (pH 7.0 and 0.1 M)

Electric stimuli response comparison between the prepared hydrogels

Figure 7a–c displays the influences of ionic strength, pH and electric voltage on the electric sensitivity of the prepared hydrogels GL4.0/SA1.6, GL4.0/SA1.2/PCMC0.4 and GL4.0/SA0.8/PCMC0.8 respectively. As shown in Fig. 7a, after applying an electric field, the maximum equilibrium bending angle of the prepared hydrogels occurred at 0.05 M of ionic strength. Lower or higher ionic strength could induce the decrease of equilibrium bending angle. At low

ionic strength, higher electrolyte concentration could lead to more free ions moving from the surrounding solution to counter-electrodes or hydrogels network. Consequently, the osmotic pressure differences between the anode and cathode of the hydrogels network could increase, finally resulting in an increased equilibrium bending angel (Lin et al. 2009). However, when the ionic strength of the solution is greater than the critical concentration, a shielding effect of the polyions can arise due to the increase of ions in the electrolytic solute, consequently resulting in a reduced electrostatic repulsion of the polyions and a decreased equilibrium bending angel (Shang et al. 2008). Similar behaviors were also reported by Shang et al. (2008) in chitosan/carboxymethyl cellulose hydrogel and Tian et al. (2010) in soy protein isolate hydrogel. The effect of pH on the electric sensitivity of the prepared hydrogels is depicted in Fig. 7b. Compared with the small bending angel in acidic solution (pH 2.0), the hydrogels showed an obviously increased bending angel in neutral (pH 7.0) or basic solutions (pH 12.0). As already described in Fig. 6, the prepared hydrogels showed a low swelling ratio at pH 2.0 and thereby formed a compact and dense structure that is adverse to the migration of charge. These behaviors could be ascribed to the formation of hydrogen bonds in the hydrogels network. However, as the increase of pH, more and more –COOH groups in the hydrogels were ionized to –COO– so that the hydrogels became less compact and the swelling ratio increased (Bekin et al. 2014), finally leading to the increased bending behavior toward the cathode. As can be observed in Fig. 7c, the equilibrium bending angle evidently increased with an increase in applied electric voltage across the hydrogels, indicating the bending behavior was induced by the electric field. Compared with the bending angel at 5 V, the bending angels of GL4.0/SA1.6, GL4.0/SA1.2/PCMC0.4 and GL4.0/SA0.8/PCMC0.8 were significantly increased 6.5, 6.4 and 5.8 times respectively at 25 V. The electric field provided the power for the electric sensitive hydrogels to bend in electrolyte solution. More the electric voltage increased, faster the ions in the solution migrated, thereby generating an ionic gradient more quickly and finally leading to an increase in bending angle (Shang et al. 2008). Similar results were also reported in the literatures (Kim et al. 2006; Shang et al. 2008; Tian et al. 2010; Tungkavet et al. 2015). Figure 7d shows the reversible bending behavior of the prepared hydrogels by alternately applying electric voltage of 25 V every 30 s. As electric field turned on and off, the hydrogels bended and returned to the initial position quickly, exhibiting perfect reversible bending behavior. Based on these reversibility and natural biocompatibility and non-toxicity, the prepared hydrogels have potential applications such as microsensors, actuators and artificial muscles. Furthermore, as can be clearly observed from Fig. 7 that an enhanced electric responsive behavior was observed by increase of bending angel as PCMC content in the hydrogels was increased. As already displayed in Fig. 3d–f (SEM images) and Figs. 4, 5, and 6 (swelling capacity), addition of PCMC could lead to the formation of hole-shaped surface and improve the swelling and responsive properties of the hydrogels, which may be attributed to the abundance of highly hydrophilic hydroxyl groups and carboxymethyl groups of PCMC (Chang et al. 2010).

Conclusion

This works synthesized natural polymer hydrogels based on gelatin, sodium alginate and pineapple peel carboxymethyl cellulose using $CaCl_2$ and glutaraldehyde as cross-linking agents. The FTIR and XRD results confirmed the presence of strong interactions among GL, SA and PCMC by hydrogen bonds. The SEM images indicated that addition of PCMC contributed to the formation of a hole-shaped structure on the hydrogels surface. The swelling dynamic mechanism of the prepared hydrogels accorded well with the Fickian diffusion model and the Schott's second-order-kinetic model. The hydrogels revealed obvious intelligent responsive behaviors to pH, salt and electric field. The hydrogels showed a stable reversible bending behavior with the repeated on–off switching of the electric field, and the electric responsive was influenced by pH, electric voltage and ionic strength. Based on these results, the prepared hydrogels possess the potential applications in the fields such as technologies as robot, sensor, artificial muscle, drug delivery system and so on.

Acknowledgments This work was supported by the National Natural Science Foundation of China under Grant Number 31471673 and 31271978.

References

Badawy ME, Taktak NE, Awad OM, Elfiki SA, El-Ela NEA (2017) Preparation and characterization of biopolymers chitosan/alginate/gelatin gel spheres crosslinked by glutaraldehyde. J Macromol Sci B 56:359–372. https://doi.org/10.1080/00222348.2017.1316640

Bekin S, Sarmad S, Gürkan K, Ke Eli GN, Gürda G (2014) Synthesis, characterization and bending behavior of electroresponsive sodium alginate/poly(acrylic acid) interpenetrating network films under an electric field stimulus. Sens Actuators B Chem 202:878–892. https://doi.org/10.1016/j.snb.2014.06.051

Chang C, Duan B, Cai J, Zhang L (2010) Superabsorbent hydrogels based on cellulose for smart swelling and controllable delivery. Eur Polym J 46:92–100. https://doi.org/10.1016/j.eurpolymj.2009.04.033

Constantin M, Bucatariu S, Doroftei F, Fundueanu G (2017) Smart composite materials based on chitosan microspheres embedded in thermosensitive hydrogel for controlled delivery of drugs. Carbohydr Polym 157:493–502. https://doi.org/10.1016/j.carbpol.2016.10.022

Dai H, Huang H (2016) Modified pineapple peel cellulose hydrogels embedded with sepia ink for effective removal of methylene blue. Carbohydr Polym 148:1–10. https://doi.org/10.1016/j.carbpol.2016.04.040

Dai H, Huang H (2017a) Enhanced swelling and responsive properties of pineapple peel carboxymethyl cellulose-g-poly(acrylic acid-co-acrylamide) superabsorbent hydrogel by the introduction of carclazyte. J Agric Food Chem 65:565–574. https://doi.org/10.1021/acs.jafc.6b04899

Dai H, Huang H (2017b) Synthesis, characterization and properties of pineapple peel cellulose-g-acrylic acid hydrogel loaded with kaolin and sepia ink. Cellulose 24:69–84. https://doi.org/10.1007/s10570-016-1101-0

Dai H, Ou S, Liu Z, Huang H (2017) Pineapple peel carboxymethyl cellulose/polyvinyl alcohol/mesoporous silica SBA-15 hydrogel composites for papain immobilization. Carbohydr Polym 169:504–514. https://doi.org/10.1016/j.carbpol.2017.04.057

de Almeida JM, de Lima VA, de Lima PCG, Knob A (2016) Effective and low-cost saccharification of pineapple peel by *Trichoderma viride* crude extract with enhanced β-glucosidase activity. Bioenergy Res 9:701–710. https://doi.org/10.1007/s12155-016-9714-6

Devi N, Kakati DK (2013) Smart porous microparticles based on gelatin/sodium alginate polyelectrolyte complex. J Food Eng 117:193–204. https://doi.org/10.1016/j.jfoodeng.2013.02.018

Dong Z, Wang Q, Du Y (2006) Alginate/gelatin blend films and their properties for drug controlled release. J Membr Sci 280:37–44. https://doi.org/10.1016/j.memsci.2006.01.002

Foo KY, Hameed BH (2012) Porous structure and adsorptive properties of pineapple peel based activated carbons prepared via microwave assisted KOH and K_2CO_3 activation. Microporous Mesoporous Mater 148:191–195. https://doi.org/10.1016/j.micromeso.2011.08.005

Gou M, Qu X, Zhu W, Xiang M, Yang J, Zhang K, Wei Y, Chen S (2014) Bio-inspired detoxification using 3D-printed hydrogel nanocomposites. Nat Commun 5:3774. https://doi.org/10.1038/ncomms4774

Hu K, Hu X, Zeng L, Zhao M, Huang H (2010) Hydrogels prepared from pineapple peel cellulose using ionic liquid and their characterization and primary sodium salicylate release study. Carbohydr Polym 82:62–68. https://doi.org/10.1016/j.carbpol.2010.04.023

Hu X, Wang J, Huang H (2013) Impacts of some macromolecules on the characteristics of hydrogels prepared from pineapple peel cellulose using ionic liquid. Cellulose 20:2923–2933. https://doi.org/10.1007/s10570-013-0075-4

Huang Y, Zhang B, Xu G, Hao W (2013) Swelling behaviours and mechanical properties of silk fibroin-polyurethane composite hydrogels. Compos Sci Technol 84:15–22. https://doi.org/10.1016/j.compscitech.2013.05.007

Ibrahim SM, Abou El Fadl FI, El-Naggar AA (2014) Preparation and characterization of crosslinked alginate-CMC beads for controlled release of nitrate salt. J Radioanal Nucl Chem 299:1531–1537. https://doi.org/10.1007/s10967-013-2820-4

Işiklan N (2006) Controlled release of insecticide carbaryl from sodium alginate, sodium alginate/gelatin, and sodium alginate/sodium carboxymethyl cellulose blend beads crosslinked with glutaraldehyde. J Appl Polym Sci 99:1310–1319. https://doi.org/10.1002/app.22012

Jana S, Banerjee A, Sen KK, Maiti S (2016) Gelatin-carboxymethyl tamarind gum biocomposites: in vitro characterization & anti-inflammatory pharmacodynamics. Mater Sci Eng C Mater 69:478–485. https://doi.org/10.1016/j.msec.2016.07.008

Kim SJ, Kim MS, Kim SI, Spinks GM, Kim BC, Wallace GG (2006) Self-oscillatory actuation at constant DC voltage with pH-sensitive chitosan/polyaniline hydrogel blend. Chem Mater 18:5805–5809. https://doi.org/10.1021/cm060988h

Lanthong P, Nuisin R, Kiatkamjornwong S (2006) Graft copolymerization, characterization, and degradation of cassava starch-g-acrylamide/itaconic acid superabsorbents. Carbohydr Polym 66:229–245. https://doi.org/10.1016/j.carbpol.2006.03.006

Lima-Tenório MK, Tenório-Neto ET, Guilherme MR, Garcia FP, Nakamura CV, Pineda EAG, Rubira AF (2015) Water transport properties through starch-based hydrogel nanocomposites responding to both pH and a remote magnetic field. Chem Eng J 259:620–629. https://doi.org/10.1016/j.cej.2014.08.045

Lin J, Tang Q, Hu D, Sun X, Li Q, Wu J (2009) Electric field sensitivity of conducting hydrogels with interpenetrating polymer network structure. Colloid Surf A 346:177–183. https://doi.org/10.1016/j.colsurfa.2009.06.011

Lin R, Li A, Lu L, Cao Y (2015) Preparation of bulk sodium carboxymethyl cellulose aerogels with tunable morphology. Carbohydr Polym 118:126–132. https://doi.org/10.1016/j.carbpol.2014.10.075

Mahdavinia GR, Mousanezhad S, Hosseinzadeh H, Darvishi F, Sabzi M (2016) Magnetic hydrogel beads based on PVA/sodium alginate/laponite RD and studying their BSA adsorption. Carbohydr Polym 147:379–391. https://doi.org/10.1016/j.carbpol.2016.04.024

Mas Haris MRH, Raju G (2014) Preparation and characterization of biopolymers comprising chitosan-grafted-ENR via acid-induced reaction of ENR50 with chitosan.

J Macromol Sci B 8:85–94. https://doi.org/10.3144/expresspolymlett.2014.11

Mu C, Guo J, Li X, Lin W, Li D (2012) Preparation and properties of dialdehyde carboxymethyl cellulose crosslinked gelatin edible films. Food Hydrocoll 27:22–29. https://doi.org/10.1016/j.foodhyd.2011.09.005

Piao Y, Chen B (2017) Synthesis and mechanical properties of double cross-linked gelatin-graphene oxide hydrogels. Int J Biol Macromol 101:791–798. https://doi.org/10.1016/j.ijbiomac.2017.03.155

Rattanapoltee P, Kaewkannetra P (2014) Utilization of agricultural residues of pineapple peels and sugarcane bagasse as cost-saving raw materials in *Scenedesmus acutus* for lipid accumulation and biodiesel production. Appl Biochem Biotechnol 173:1495–1510. https://doi.org/10.1007/s12010-014-0949-4

Ren H, Gao Z, Wu D, Jiang J, Sun Y, Luo C (2016) Efficient Pb(II) removal using sodium alginate-carboxymethyl cellulose gel beads: preparation, characterization, and adsorption mechanism. Carbohydr Polym 137:402–409. https://doi.org/10.1016/j.carbpol.2015.11.002

Saarai A, Kasparkova V, Sedlacek T, Saha P (2013) On the development and characterisation of crosslinked sodium alginate/gelatine hydrogels. J Mech Behav Biomed 18:152–166. https://doi.org/10.1016/j.jmbbm.2012.11.010

Saelo S, Assatarakul K, Sane A, Suppakul P (2016) Fabrication of novel bioactive cellulose-based films derived from caffeic acid phenethyl ester-loaded nanoparticles via a rapid expansion process: RESOLV. J Agric Food Chem 64:6694–6707. https://doi.org/10.1021/acs.jafc.6b0219

Samanta HS, Ray SK (2014) Synthesis, characterization, swelling and drug release behavior of semi-interpenetrating network hydrogels of sodium alginate and polyacrylamide. Carbohydr Polym 9:666–678. https://doi.org/10.1016/j.carbpol.2013.09.004

Schott H (1992) Swelling kinetics of polymers. J Macromol Sci B 31:1–9. https://doi.org/10.1080/00222349208215453

Shang J, Shao Z, Chen X (2008) Electrical behavior of a natural polyelectrolyte hydrogel: chitosan/carboxymethylcellulose hydrogel. Biomacromolecules 9:1208–1213. https://doi.org/10.1021/bm701204j

Shi X, Zheng Y, Wang C, Yue L, Qiao K, Wang G, Wang L, Quan H (2015) Dual stimulus responsive drug release under the interaction of pH value and pulsatile electric field for a bacterial cellulose/sodium alginate/multi-walled carbon nanotube hybrid hydrogel. RSC Adv 5:41820–41829. https://doi.org/10.1039/C5RA04897D

Sommer S, Dickescheid C, Harbertson JF, Fischer U, Cohen SD (2016) Rationale for haze formation after carboxymethyl cellulose (CMC) addition to red wine. J Agric Food Chem 64:6879–6887. https://doi.org/10.1021/acs.jafc.6b02479

Tang H, Chen H, Duan B, Lu A, Zhang L (2014) Swelling behaviors of superabsorbent chitin/carboxymethylcellulose hydrogels. J Mater Sci 49:2235–2242. https://doi.org/10.1007/s10853-013-7918-0

Thakur VK, Thakur MK, Gupta RK (2014) Graft copolymers of natural fibers for green composites. Carbohydr Polym 104:87–93. https://doi.org/10.1016/j.carbpol.2014.01.016

Thu H, Ng S (2013) Gelatine enhances drug dispersion in alginate bilayer film via the formation of crystalline microaggregates. Int J Pharm 454:99–106. https://doi.org/10.1016/j.ijpharm.2013.06.082

Tian K, Shao Z, Chen X (2010) Natural electroactive hydrogel from soy protein isolation. Biomacromolecules 11:3638–3643. https://doi.org/10.1021/bm101094g

Tungkavet T, Seetapan N, Pattavarakorn D, Sirivat A (2015) Electromechanical properties of multi-walled carbon nanotube/gelatin hydrogel composites: effects of aspect ratios, electric field, and temperature. Mater Sci Eng C Mater 46:281–289. https://doi.org/10.1016/j.msec.2014.10.068

Ullah F, Othman MBH, Javed F, Ahmad Z, Md Akil H (2015) Classification, processing and application of hydrogels: a review. Mater Sci Eng C Mater 57:414–433. https://doi.org/10.1016/j.msec.2015.07.053

Wan J, Guo J, Miao Z, Guo X (2016) Reverse micellar extraction of bromelain from pineapple peel—effect of surfactant structure. Food Chem 197:450–456. https://doi.org/10.1016/j.foodchem.2015.10.145

Wang A, Wang W, Wang J, Kang Y (2011) Synthesis, swelling and responsive properties of a new composite hydrogel based on hydroxyethyl cellulose and medicinal stone. Compos Part B Eng 42:809–818. https://doi.org/10.1016/j.compositesb.2011.01.018

Yadav M, Rhee KY, Park SJ (2014) Synthesis and characterization of graphene oxide/carboxymethylcellulose/alginate composite blend films. Carbohydr Polym 110:18–25. https://doi.org/10.1016/j.carbpol.2014.03.037

Yu Z, Cai Z, Chen Q, Liu M, Ye L, Ren J, Liao W, Liu S (2016) Engineering β-sheet peptide assemblies for biomedical applications. Biomater Sci 4:365–374. https://doi.org/10.1039/C5BM00472A

Zhang W, Zhu S, Bai Y, Xi N, Wang S, Bian Y, Li X, Zhang Y (2015) Glow discharge electrolysis plasma initiated preparation of temperature/pH dual sensitivity reed hemicellulose-based hydrogels. Carbohydr Polym 122:11–17. https://doi.org/10.1016/j.carbpol.2015.01.007

Zhang H, Yang M, Luan Q, Tang H, Huang F, Xiang X, Yang C, Bao Y (2017) Cellulose anionic hydrogels based on cellulose nanofibers as natural stimulants for seed germination and seedling growth. J Agric Food Chem 65:3785–3791. https://doi.org/10.1021/acs.jafc.6b05815

Zhao S, Yao S, Ou S, Lin J, Wang Y, Peng X, Li A, Yu B (2013) Preparation of ferulic acid from corn bran: its improved extraction and purification by membrane separation. Food Bioprod Process 92:309–313. https://doi.org/10.1016/j.fbp.2013.09.004